

Dynamical analysis of $R \frac{1}{\square^2} R$ cosmology: Impact of initial conditions and constraints from supernovae

Henrik Nersisyan,^{1,*} Yashar Akrami,^{1,†} Luca Amendola,^{1,‡} Tomi S. Koivisto,^{2,§} and Javier Rubio^{1,¶}

¹*Institut für Theoretische Physik, Ruprecht-Karls-Universität Heidelberg, Philosophenweg 16, 69120 Heidelberg, Germany*

²*Nordita, KTH Royal Institute of Technology and Stockholm University, Roslagstullsbacken 23, 10691 Stockholm, Sweden*

(Dated: July 10, 2018)

We discuss the cosmological implications of the $R \square^{-2} R$ nonlocal modification to standard gravity. We relax the assumption of special initial conditions in the local formulation of the theory, perform a full phase-space analysis of the system, and show that the late-time cosmology of the model exhibits two distinct evolution paths, on which a large range of values for the present equation of state can be reached. We then compare the general solutions to supernovae data and place constraints on the parameters of the model. In particular, we find that the mass parameter of the theory should be smaller than 1.2 in Hubble units.

Keywords: modified gravity, nonlocal gravity, dark energy, background cosmology

I. INTRODUCTION

The current standard model of cosmology, called Λ CDM (CDM for cold dark matter), cannot be reconciled with general relativity (GR) and the Standard Model of particle physics without extreme fine-tuning. In particular, the ratio $\sqrt{\Lambda}/M_{\text{Pl}}^2$ derived from observations [with Λ the notorious cosmological constant (CC) and M_{Pl} the reduced Planck mass] is almost infinitesimal compared to the value obtained by the most straightforward extrapolations of GR and quantum field theory, to the infrared scale $\sqrt{\Lambda}/M_{\text{Pl}}$ and high-energy scales approaching M_{Pl} , respectively. This calls both for the observational pursuit of signatures that could provide hints on the possible physics beyond the Λ CDM model, and for theoretical extensions that could explain the cosmological data in a more natural way [1, 2].

Various attempts at such extensions have been undertaken in the context of nonlocal gravity [3, 4]. In a top-bottom approach, the possibility that gravitational interactions become nonlocal near the Planck scale is suggested, among others, by string theory [5, 6]. From a bottom-up perspective, nonlocal theories are appealing because of their potential to provide an ultraviolet completion of the metric gravity theory [7–9], but there are also motivations to contemplate nonlocal terms in the infrared as well. Such infrared nonlocal terms arise generically in effective field theories after integrating out light degrees of freedom [4, 10, 11], but may also feature in more fundamental actions in Euclidean quantum gravity [12, 13]. Nonlocal effective formulations have been found for gravity models with a massive graviton [14, 15], multiple metrics [16], and post-Riemannian, affine geometry [17]. In passing, we note that indeed the recent development of a conformal affine gauge theory of gravity [18] introduces a novel holography that, along the lines of Ref. [19], may naturally provide a nonlocal link between the value of the cosmological constant and the amount of information contained in the emergent spacetime.

Nonlocal gravity models are typically written as an Einstein-Hilbert term supplemented with integral or infinite-derivative curvature terms. The first proposal for a nonlocal dark-energy model was put forward by Deser and Woodard (DW) and has the form [20]

$$\mathcal{L}^{\text{DW}} = \frac{M_{\text{Pl}}^2}{2} R \left[1 - f \left(\frac{R}{\square} \right) \right], \quad (1)$$

where R is the Ricci curvature scalar and $1/\square$ is the inverse d'Alembertian, an integral operator such that $\square(1/\square) = 1$, with $\square \equiv g^{\mu\nu} \nabla_\mu \nabla_\nu$ and ∇_μ the Christoffel covariant derivative. With the dimensionless combination R/\square , one could in principle construct models without introducing new scales. The integral dependence of the corrections could generate the observed acceleration at the present cosmological epoch dynamically and without special fine-tunings. However, detailed investigations have shown that, although the function f can be chosen in such a way that the background expansion is consistent with the data [21–23] and the model has a viable Newtonian limit [24, 25], the

* h.nersisyan@thphys.uni-heidelberg.de

† y.akrami@thphys.uni-heidelberg.de

‡ l.amendola@thphys.uni-heidelberg.de

§ tomi.koivisto@nordita.org

¶ j.rubio@thphys.uni-heidelberg.de

impact of the nonlocal corrections on the evolution of perturbations is strong and utterly rules the model out when this is confronted with large-scale structure data [26]. On top of that, nonlocal modifications of gravity result generically in instabilities at the level of perturbations, at least if they involve tensorial terms such as $(W_{\mu\nu\rho\sigma}/\square^2)W^{\mu\nu\rho\sigma}$ [27] with $W_{\mu\nu\rho\sigma}$ the Weyl tensor appearing in models inspired by the conformal anomaly [28, 29].

One of the remarkable features of the model

$$\mathcal{L}^{\text{MM}} = \frac{M_{\text{Pl}}^2}{2} R \left[1 - \frac{m^2}{6} \left(\frac{1}{\square} \right)^2 R \right] = \frac{M_{\text{Pl}}^2}{2} \left[R - \frac{m^2}{6} \left(\frac{R}{\square} \right)^2 \right], \quad (2)$$

proposed by Maggiore and Mancarella (MM) [30] is that it can produce nonlocal dark energy able to fit the background data while retaining a matter power spectrum compatible with observations (see Refs. [31–34] and [35–38] for studies of the background expansion and of structure formation, respectively). It is also notable that the $(R/\square)^2$ -correction to GR has indeed been obtained in an effective field theory for gravity at the second order curvature expansion¹ [10] and that the MM model appears to have only one new parameter m at the level of the gravitational Lagrangian, i.e. none more than Λ CDM.² It has also been argued that ghost fields do not destabilize the model [30] (see also Ref. [40]). Spherically symmetric solutions have also been considered [25, 41].

In this paper, we study the cosmological dynamics of the MM model, with special attention to the problem of initial conditions. Nonlocal theories with infinite order derivative operators require the specification of an infinite number of initial conditions for the formulation of the Cauchy problem. Analogously, nonlocal integral operators, such as the one featured in the MM model, are strictly defined only by specifying the boundary conditions for each of the infinite number of modes in the continuum limit of the Fourier space. Various techniques have been considered to deal with such theories, see Refs. [42–49]. The MM model (2) can be reformulated in terms of two scalar fields [24], which should not be considered however as local dynamical fields evolving freely in time, but as auxiliary fields whose configuration at each spatial hypersurface is dictated by the other fields and the boundary conditions of the $1/\square$ -operator. In the phase space of the homogeneous cosmological dynamics, the trajectories of the two (fake) scalar degrees of freedom are uniquely fixed given four numbers at any given cosmological epoch. The cosmology of the MM model seems to offer a natural or “minimal” assumption for the choice of these numbers: at a sufficiently early epoch in the standard cosmology, the Universe is filled with radiation only, for which $R \approx 0$. It therefore seems an obvious choice to set $R/\square = R/\square^2 = 0$ at such an epoch.³ However, already at the linear order in the inhomogeneous fluctuations, both the inverse- and the double-inverse-d’Alembertian operators bring forth scale-dependent functions in the momentum space. Unless finely adjusted and compensating scale dependence is encoded into the boundary conditions of the $1/\square$ -operators, the initial conditions for cosmological perturbations would feature additional scale dependence (compared to Λ CDM). The minimal boundary conditions, that is $\delta(R/\square) = 0$ when $\delta R = 0$ (we denote perturbations with δ), would require scale dependence in the initial conditions for the auxiliary fields. An important point is that due to their assumed nonlocal origin, they impose constraints rather than adding dynamics. Thus one expects the nonminimal scale dependence of the initial conditions to be directly projected (or, if set in terms of the auxiliary fields, to effectively propagate) to the smaller redshifts of the crucial observables, where especially the matter power spectrum is very sensitive to the possible scale dependence in the dark sector, as that is reflected through the gravitational interaction in the baryon distribution. Since the confrontation with large-scale structure is crucial for distinguishing the MM (2) and the earlier proposal (1), the issue of (scale-dependent) linear boundary conditions calls for clarification.

In this paper we undertake a comprehensive study of the expansion dynamics in the MM model. In Sec. II we rewrite the model (2) in terms of two (effective) auxiliary scalar fields, and set up the phase space spanned by convenient dimensionless variables whose dynamical system can be closed into an autonomous form. In Sec. III we perform a full dynamical system analysis in order to identify the critical points in the cosmological phase space and determine their stability. Each set of initial conditions fixes a trajectory in the phase space, corresponding to a particular family of MM models with the same mass parameter m and the same four cosmological background boundary conditions. By exploring the global structure of the phase space we can thus map the cosmology of different models and investigate the sensitivity of the predictions to changing the parameters of the model (i.e. to the initial conditions that have been previously assumed minimal). In Sec. IV we confront the model with supernovae data constraining the background expansion, in such a way that we do not fix all the initial conditions but marginalize over them. Our findings are then summarized in Sec. V.

¹ As shown in Ref. [39], the coefficient of the $R\square^{-2}R$ obtained by this procedure should satisfy $M^2/H^2 \ll 1$ with $M^4 \sim (M_{\text{Pl}} m)^2$. Unfortunately, this condition is not compatible with the value of m required to obtain a realistic cosmology ($m \sim H_0$).

² Expectedly, viable dark energy models require $m \sim \Lambda/M_{\text{Pl}} \sim H_0$, where H_0 is the present Hubble rate.

³ Note however that the cosmology obviously depends on the thermal history. In Appendix B, we check the impact of setting $R/\square = R/\square^2 = 0$ either at the matter-radiation equality or at an earlier period.

II. THE COSMOLOGY OF $R\frac{1}{\square^2}R$ GRAVITY MODEL

The full action, including both gravity and matter sectors, for the MM nonlocal theory introduced in Eq. (2) has the form

$$S^{\text{MM}} = \frac{M_{\text{Pl}}^2}{2} \int d^4x \sqrt{-g} \left(R - \frac{m^2}{6} R \frac{1}{\square^2} R \right) + \int d^4x \sqrt{-g} \mathcal{L}_m, \quad (3)$$

with the mass scale m the only free parameter of the theory, to be determined observationally, and \mathcal{L}_m the matter Lagrangian minimally coupled to gravity.

In order to derive the modified Einstein equations, we vary the action (3) with respect to the metric $g_{\mu\nu}$:

$$\begin{aligned} \delta S^{\text{MM}} &= \frac{M_{\text{Pl}}^2}{2} \int d^4x \delta(\sqrt{-g}) \left(R - \frac{m^2}{6} R \frac{1}{\square^2} R \right) \\ &+ \frac{M_{\text{Pl}}^2}{2} \int d^4x \sqrt{-g} \left(\delta R - \frac{m^2}{3} \delta R \frac{1}{\square^2} R + \frac{m^2}{3} R \frac{1}{\square} \delta \square \left(\frac{1}{\square^2} R \right) \right) + \delta \int d^4x \sqrt{-g} \mathcal{L}_m, \end{aligned} \quad (4)$$

where we have used $\delta(\square^{-2}) = -2\square^{-1}(\delta\square)\square^{-2}$. Denoting the conserved stress-energy tensor of matter by T_ν^μ , the gravitational field equations turn out to be [30]

$$G_\nu^\mu - \frac{1}{6} m^2 K_\nu^\mu = 8\pi G T_\nu^\mu, \quad (5)$$

where we have defined

$$K_\nu^\mu \equiv 2SG_\nu^\mu - 2\nabla^\mu \partial_\nu S + 2\delta_\nu^\mu \square S + \delta_\nu^\mu \partial_\rho S \partial^\rho U - \frac{1}{2} \delta_\nu^\mu U^2 - (\partial^\mu S \partial_\nu U + \partial_\nu S \partial^\mu U), \quad (6)$$

and introduced the two auxiliary fields U and S through the equations

$$\square U \equiv -R, \quad (7)$$

$$\square S \equiv -U. \quad (8)$$

Writing the field equations in terms of U and S allows us to work with a local formulation of the theory [30]. In order to solve Eq. (5) we need to first solve Eqs. (7) and (8). The general solutions for U and S are given by

$$U \equiv U_{\text{hom}} - \square_{\text{ret}}^{-1} R, \quad (9)$$

$$S \equiv S_{\text{hom}} - \square_{\text{ret}}^{-1} U, \quad (10)$$

with U_{hom} and S_{hom} the solutions to the homogeneous equations

$$\square U_{\text{hom}} = 0, \quad \square S_{\text{hom}} = 0, \quad (11)$$

and $\square_{\text{ret}}^{-1}$ the inverse of the retarded d'Alembertian operator. The equivalent local form of the theory then depends on the choice of U_{hom} and S_{hom} . The *ad hoc* choice of a retarded Green function in the definition of inverse d'Alembertian operator \square^{-1} will ensure causality (for details see e.g. Ref. [49]). Note, however, that it has been argued that causality can emerge automatically if one considers only in-in (observable) vacuum expectation values [40, 50, 51].

Let us now turn to our studies of the cosmology of the model. We will assume a flat Friedmann-Lemaître-Robertson-Walker (FLRW) metric

$$ds^2 = -dt^2 + a^2(t) d\vec{x}^2, \quad (12)$$

with t the cosmic time and a the scale factor.

Solving the field equations for this metric yields the evolution equations (equivalent to the Friedmann equation) [30]

$$h^2 = \frac{\Omega_{\text{M}}^0 e^{-3N} + \Omega_{\text{R}}^0 e^{-4N} + (\gamma/4) U^2}{1 + \gamma(-3V - 3V' + (1/2)V'U')}, \quad (13)$$

$$U'' = 6(2 + \xi) - (3 + \xi)U', \quad (14)$$

$$V'' = h^{-2}U - (3 + \xi)V', \quad (15)$$

in terms of the auxiliary fields U and $V \equiv H_0^2 S$, and their derivatives, with H_0 the present Hubble rate. Additionally, we have assumed the Universe to be filled with matter and radiation, with present density parameters Ω_M^0 and Ω_R^0 , respectively, and have defined the quantities

$$\gamma \equiv \frac{m^2}{9H_0^2}, \quad h \equiv \frac{H}{H_0}, \quad \xi \equiv \frac{h'}{h}, \quad (16)$$

where a prime denotes a derivative with respect to the number of e -foldings $N \equiv \ln a$.

The evolution of the total energy density can be parametrized in terms of an effective equation of state [1]

$$w_{\text{eff}} = -1 - \frac{2}{3} \frac{h'}{h} = -1 - \frac{2}{3} \xi. \quad (17)$$

The evolutions of the matter, radiation and dark energy components contributing to w_{eff} follow from the conservation of the energy-momentum tensor,

$$\Omega_M' + (3 + 2\xi) \Omega_M = 0, \quad \Omega_R' + (4 + 2\xi) \Omega_R = 0, \quad \Omega_{\text{DE}}' + (3 + 3w_{\text{DE}} + 2\xi) \Omega_{\text{DE}} = 0, \quad (18)$$

with

$$\xi = \frac{-4\Omega_R - 3\Omega_M + 3\gamma(h^{-2}U + U'V' - 4V')}{2(1 - 3\gamma V)}. \quad (19)$$

Combining the conservation equations (18) and taking into account the cosmic sum rule,

$$\Omega_{\text{DE}} = 1 - h^{-2}(\Omega_M^0 e^{-3N} + \Omega_R^0 e^{-4N}) = \gamma \left(\frac{1}{4} h^{-2} U^2 + 3V + 3V' - \frac{1}{2} V' U' \right), \quad (20)$$

we obtain the dark energy equation of state,

$$w_{\text{DE}} = \frac{\gamma(4(U+3) - (U+2)U')V' + U(\gamma V(\Omega_R + 3) - \Omega_{\text{DE}}) + 4(3\gamma V - \Omega_{\text{DE}})}{U(1 - 3\gamma V)\Omega_{\text{DE}}}. \quad (21)$$

III. PHASE SPACE AND DYNAMICAL ANALYSIS

In order to perform the dynamical analysis of the model, it is convenient to rewrite the second order differential equations (14) and (15) in a first order form. To do this, we introduce two new fields Y_1 and Y_2 defined as $Y_1 \equiv U'$ and $Y_2 \equiv V'$. We can now rewrite the system as a set of six autonomous first order differential equations

$$U' = Y_1, \quad (22)$$

$$V' = Y_2, \quad (23)$$

$$Y_1' = -\frac{3((U+2)Y_1 - 4(U+3))(2(3\gamma V - 1) - \gamma(Y_1 - 6)Y_2) + 3(U+4)(Y_1 - 6)\Omega_M + 4(U+3)(Y_1 - 6)\Omega_R}{2U(3\gamma V - 1)}, \quad (24)$$

$$Y_2' = -\frac{Y_2(6(3\gamma V - 1) - 3\gamma(Y_1 - 4)Y_2 + 3\Omega_M + 4\Omega_R)}{2(3\gamma V - 1)} \quad (25)$$

$$-\frac{(2(3\gamma V - 1) + 3\gamma Y_2)(2(3\gamma V - 1) - \gamma(Y_1 - 6)Y_2 + 2(\Omega_M + \Omega_R))}{\gamma U(3\gamma V - 1)},$$

$$\Omega_M' = -\frac{\Omega_M(U(3(3\gamma V - 1) - 3\gamma(Y_1 - 4)Y_2 + 3\Omega_M + 4\Omega_R) + 12(3\gamma V - 1) + 12(\Omega_M + \Omega_R) - 6\gamma(Y_1 - 6)Y_2)}{U(3\gamma V - 1)}, \quad (26)$$

$$\Omega_R' = -\frac{\Omega_R(U(4(3\gamma V - 1) - 3\gamma(Y_1 - 4)Y_2 + 3\Omega_M + 4\Omega_R) + 12(3\gamma V - 1) + 12(\Omega_M + \Omega_R) - 6\gamma(Y_1 - 6)Y_2)}{U(3\gamma V - 1)}. \quad (27)$$

A quick look at Eqs. (22)-(27) reveals that they are not invariant under $U \rightarrow U + U_{\text{hom}}$ and $\rho \rightarrow \rho + \Lambda$, where ρ is the energy density of the system. Contrary to the nonlocal models considered in Ref. [40], non-zero and constant values of U_{hom} are not equivalent to a cosmological constant. The main purpose of this work is a complete characterization of the system (22)-(27) for arbitrary values of U_{hom} and V_{hom} . As argued in Ref. [30], each choice of U_{hom} and V_{hom} in Eq. (11) (note that S and V are the same up to a constant factor) corresponds to the choice of one and only one boundary condition in the nonlocal formulation of the theory. Different initial conditions, and therefore different solutions, should be associated with different nonlocal models. The qualitative analysis of Eqs. (13)-(15) will allow us to understand which of these models are phenomenologically viable.

Point	U	V	U'	V'	Ω_M	Ω_R	w_{eff}	Type
I	\tilde{U}	$(1 - \tilde{\Omega}_R)/(3\gamma)$	0	0	0	$\tilde{\Omega}_R$	1/3	Saddle
II	$2N + \tilde{U}$	$(1 - \tilde{\Omega}_M)/(3\gamma)$	2	0	$\tilde{\Omega}_M$	0	0	Saddle
III	$+\infty$	$1/(3\gamma)$	4	0	0	0	-1	Attractor
IV	$4N + \tilde{U}$	$\pm\infty$	4	$\pm\infty$	0	0	-1	Saddle
V	-3	$\pm\infty$	0	$4V$	$\mp\infty$	0	1/3	Attractor

Table I. Critical points of the dynamical system (22)-(27). The quantities $\tilde{\Omega}_M$, $\tilde{\Omega}_R$, and \tilde{U} stand, respectively, for some constant values of Ω_M , Ω_R and U .

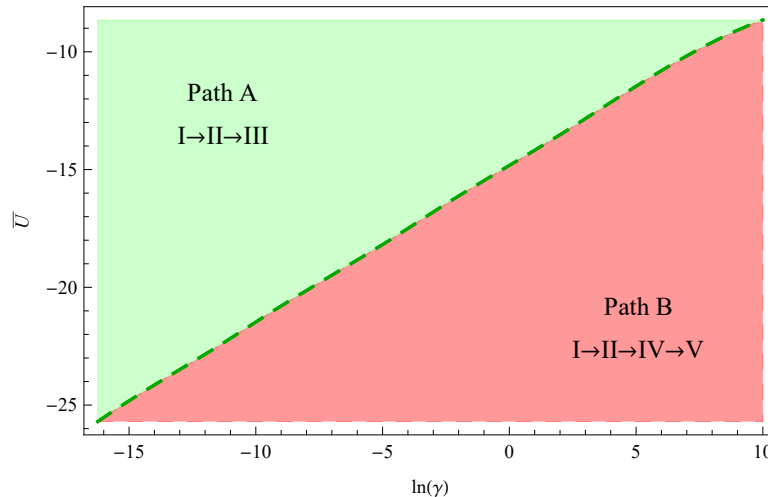


Figure 1. The two evolution paths A and B for the background cosmology of $R\Box^{-2}R$ gravity, in terms of the initial value U_0 of the auxiliary field U and the value of $\gamma \equiv \frac{m^2}{9H_0^2}$. The diagonal line depicts the critical value \tilde{U} as a function of γ . The green (red) region corresponds to the realizations of path A (B).

A. Critical points and evolution paths: Numerical analysis

The fixed points of the dynamical system (22)-(27) are those at which all the first derivatives on the left-hand side of the equations vanish. In some cases though, one can have fixed surfaces instead of fixed points, that is, only a subset of variables is constant. In order to go from the fixed surfaces to fixed points (in a lower dimensional phase space) one has to perform an appropriate variable transformation (cf. Appendix A for details regarding the treatment of fixed lines). By following this procedure, we obtain the five nontrivial fixed points/surfaces I-V listed in Table I. The values of the dynamical variables of the system (i.e. the quantities U , V , U' , V' , Ω_M , and Ω_R) are given for each point, as well as the value of the effective equation of state parameter w_{eff} . As reflected in the table, we find two attractors and three saddle points.⁴

The behavior of the solutions around each of the critical points can be determined by using the standard phase-space analysis methods. Although the set of equations (22)-(27) is nonlinear, the system behaves linearly in the vicinity of each critical point, provided that the point is isolated and the Jacobian at the point is invertible.⁵ The linearization of Eqs. (22)-(27) in the vicinity of each fixed point gives rise to a set of linear equations, which can be generically written in a matrix form $\mathbf{X}' = \mathbf{A} \cdot \mathbf{X}$, with \mathbf{A} a 6×6 matrix and $\mathbf{X} = \{U, V, U', V', \Omega_M, \Omega_R\}$. The behavior of the system around each critical point is determined by the eigenvalues of the corresponding \mathbf{A} matrix. The results are summarized in the last column of Table I (cf. Appendix A for details).

The precise interpolation of the solutions between the critical points I-V depends on the initial conditions, and in particular, on the relation between the initial value U_0 and a γ -dependent critical value \tilde{U} that we obtain numerically

⁴ One should note that for point III, Eqs. (22)-(27) may seem to be singular in the limit $V \rightarrow 1/3\gamma$. This is, however, not the case, as in the limit $V' = \Omega_M = \Omega_R = 0$ and $U' = 4$, the divergent factor is canceled out.

⁵ This argumentation holds only if the fixed point of the linearized system is not a center-type point.

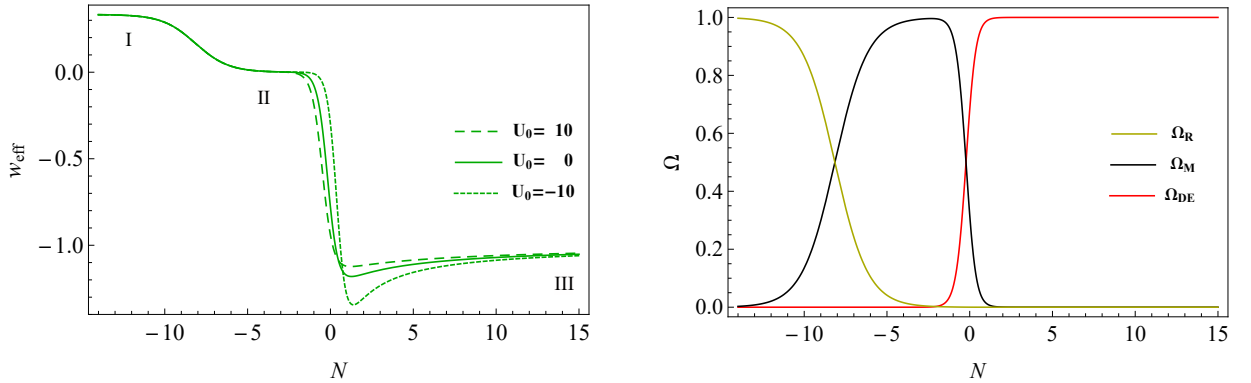


Figure 2. (Left) Evolution of the effective equation of state w_{eff} as a function of $N \equiv \ln a$ for path A. (Right) Evolution of the density parameters Ω_M, Ω_R , and Ω_{DE} for the same path with $U_0 = 0$. In both plots we have fixed $V_0 = 0$.

for the case $\Omega_M^0 = 0.3$,⁶

$$\bar{U}(\gamma) \simeq -14.82 + 0.67 \log \gamma, \quad (28)$$

and that is valid in the range illustrated in Fig. 1. We can distinguish two kinds of trajectory. If U_0 (the initial value of U) is bigger than \bar{U} , the system follows the sequence I→II→III. In the opposite case, it follows the I→II→IV→V sequence. We will refer to these two possibilities as path A and path B, respectively (see Fig. 1). The previous work on this model, i.e. Ref. [32], has focused on the particular case of path A, as we discuss in detail below.

1. Path A

The numerical behavior of the dynamical system along path A is shown in Figs. 2 and 3. Note that in Fig. 2 we have fixed $V_0 = 0$. This choice can be made without loss of generality due to the attractor behavior of point III.

As can be clearly seen in Fig. 2, the saddle points I and II correspond to intermediate radiation- and matter-dominated eras. The transition to the attractor point III proceeds through a transient phantom regime with $w_{\text{eff}} < -1$. This kind of behavior was first recognized in Ref. [32] where the authors considered the solution of the dynamical system (13)-(15) for a specific choice of the initial conditions ($U_0 = 0, V_0 = 0$) and derived a lower bound for the effective equation of state ($-1.14 \leq w_{\text{eff}} < -1$). As shown in Fig. 2, this bound is not robust under variations of the initial conditions. General choices of U_0 can lead to a stronger phantom regime (or even to its complete disappearance, cf. Sec. III A 2). Note also that the particular choice of initial conditions in the MM model rests on the assumption of a vanishing Ricci scalar prior to matter-radiation equality, or in other words, on the existence of a perfect radiation-dominated era. However, the accuracy and redshifts for which this assumption holds depend on the thermal history of the Universe. As shown in Appendix B, if the initial MM conditions were set for instance at the end of inflation/reheating, one should expect nonvanishing values of U_0 at the number of e -foldings at which the MM initial conditions are usually implemented ($N \simeq -14$) [35].

In spite of the asymptotic approach of the effective equation of state to $w_{\text{eff}} = -1$, the attractor point III *should not* be identified, *sensu stricto*, with a de Sitter point. For a solution to be de Sitter, the Hubble parameter around this solution should remain constant (or, more generally, the Ricci scalar R should be constant). This is certainly not the case here. Indeed, the Hubble rate $H(N)$ becomes infinitely large when $N \rightarrow \infty$. This unusual behavior can be easily understood by considering the consistency of Eqs. (14), (15), and (17) at the fixed point III.⁷

2. Path B

The numerical evolution of the dynamical system along path B is shown in Figs. 4 and 5. Note that in Fig. 4 we have fixed $V_0 = 0$. This can be done without loss of generality, provided that $V_0 < 1/(3\gamma) - V_0'$ (see the discussion below).

⁶ We will recover analytically the γ -dependent part of this equation in Sec. III B.

⁷ In order for Eq. (15) to be consistent at III, we must require $H \rightarrow \infty$ faster than U .

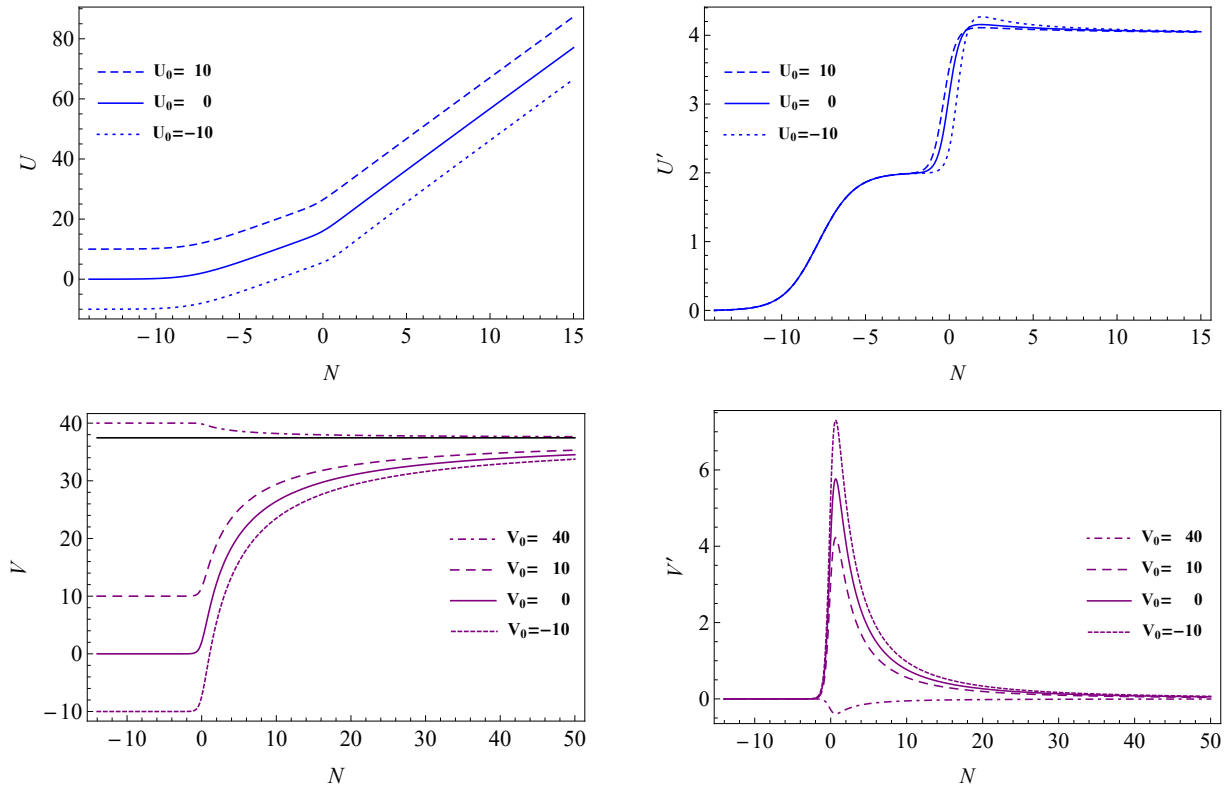


Figure 3. Evolution of the auxiliary fields U and V , and their derivatives with respect to $N \equiv \ln a$, U' and V' , for path A. In the plots of U and U' we have fixed $V_0 = 0$, and in the plots of V and V' we have fixed $U_0 = 0$.

The initial behavior of the system coincides with that in path A. In particular, the Universe undergoes radiation- and matter-dominated eras while passing through the saddle points I and II. The differences appear only when the system approaches the fixed point IV. As shown on the left-hand side of Fig. 4, this point gives rise to a *true* de Sitter epoch with $w_{\text{eff}} \simeq -1$ and $H(N) \simeq \text{constant}$. Note, however, that this point is not an attractor but rather a saddle point. This means that the solution stays close to the point for some period of time but eventually moves to the final attractor, the fixed point V. In particular, the late-time evolution depends on the value of V_0 and V'_0 . As discussed in Appendix A, if $V_0 > 1/(3\gamma) - V'_0$ then the system approaches the fixed point V with $\Omega_M \rightarrow -\infty$. Since Ω_M takes negative values when $V_0 > 1/(3\gamma) - V'_0$, this set of initial conditions should be discarded on general physical grounds. On the contrary, if $V_0 < 1/(3\gamma) - V'_0$ we can obtain a physically viable scenario. As shown on the right-hand side of Fig. 4, the matter density parameter in this case is driven to $+\infty$ while the dark energy one goes to $-\infty$. This limit is acceptable since Ω_{DE} does not represent a proper matter content but rather an effective description of the gravitational degrees of freedom. Note that the effective equation of state at point V approaches the radiation-domination value $w_{\text{eff}} = 1/3$, even though there is no radiation left.⁸

The cosmological evolution along path B requires only that $U_0 < \bar{U}$. The value of U_0 is in principle unbounded from below. Could it be possible to obtain a phantom regime similar to that occurring for path A by choosing $U_0 \ll \bar{U}$? The answer to this question turns out to be negative. As shown in Fig. 5, when we increase the absolute value of U_0 , the variable U' approaches a maximal value $U'_{\text{max}} = 4$, stays there for some time interval $\Delta N_{\text{max}}^{U'}(U_0)$, and eventually falls into its future attractor regime $U' = 0$. The maximum value of U' ($U'_{\text{max}} = 4$) translates, through Eq. (14), into a value $\xi_{\text{max}} = 0$, and as a result, $w_{\text{eff}} = -1 - \frac{2}{3}\xi$ cannot be smaller than -1 . In other words, path B is never phantom.

B. Evolution paths: Analytical results

The novel ingredient of the local formulation of the $R\Box^{-2}R$ model with respect to general relativity is the presence of two “integral fields” U and V arising from the nonlocal structure of the theory, cf. Eqs (9) and (10). In this

⁸ In fact, for all the points III, IV, and V, $\Omega_R \rightarrow 0$.

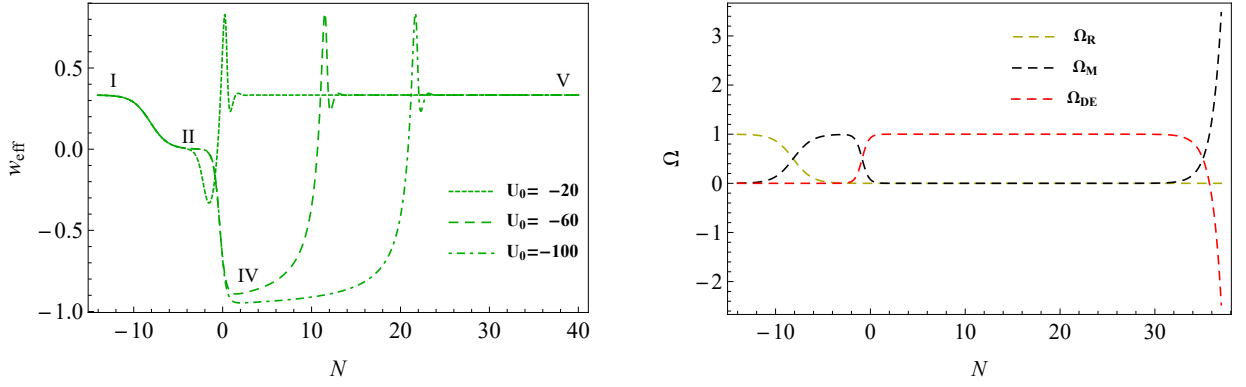


Figure 4. (Left) Evolution of the effective equation of state w_{eff} as a function of $N \equiv \ln a$ for path B. (Right) Evolution of the density parameters Ω_M , Ω_R , and Ω_{DE} for the same path with $U_0 = -60$. In both plots we have fixed $V_0 = 0$.

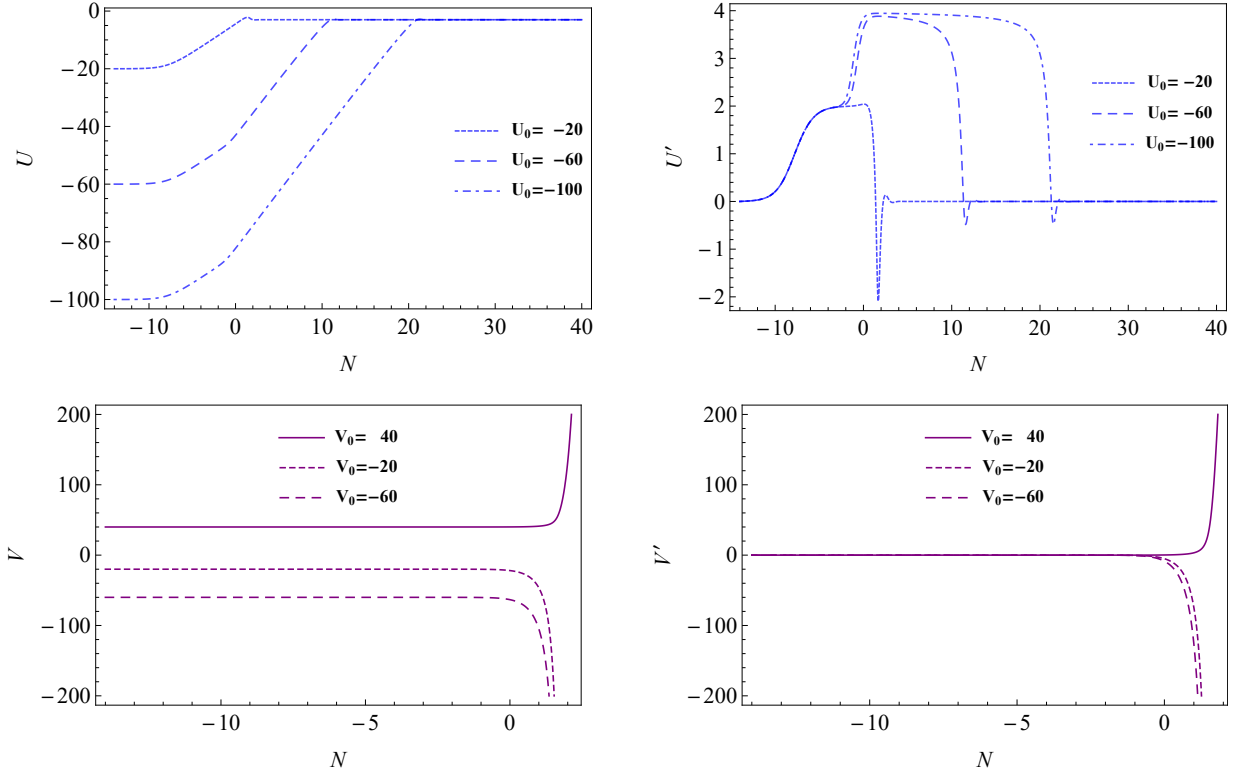


Figure 5. Evolution of the auxiliary fields U and V , and their derivatives with respect to $N \equiv \ln a$, U' and V' , for path B. In the plots of U and U' we have fixed $V_0 = 0$, and in the plots of V and V' we have fixed $U_0 = -20$.

subsection, we take an in-depth look at the evolution of the 2 + 2 homogeneous and 1 + 1 inhomogeneous modes and analytically confirm the results obtained in Secs. III A 1 and III A 2.

The basic building blocks of cosmological model construction are solutions with constant effective equation of state w_{eff} . Assuming $w_{\text{eff}} = w_c$ with w_c a constant, and using Eqs. (9) and (10), we obtain the following equations for the U and V fields

$$U(N) = u_0 + u_1 e^{-\frac{3}{2}(1-w_c)N} + \frac{2(1-3w_c)}{1-w_c} N, \quad (29)$$

$$V(N) = \frac{2e^{3(1+w_c)N}}{9(1+w_c)(3+w_c)} \left(u_0 - \frac{2(1-3w_c)(5+3w_c)}{3(1-w_c^2)(3+w_c)} - \frac{2(1-3w_c)}{1-w_c} N \right) + \frac{2e^{\frac{3}{2}(1+3w_c)N}}{9(1+w_c)(1+3w_c)} u_1 + v_0 + v_1 e^{-\frac{3}{2}(1-w_c)N}, \quad (30)$$

with u_0 , u_1 , v_0 , and v_1 ⁹ integration constants set at $N = 0$. These equations reveal that the inhomogeneous modes disappear if and only if $w_c = 1/3$. As a default, $w_c = 1/3$ is the only constant equation of state giving rise to an attractor solution.¹⁰ Note also that for $-3 < w_c < 1$ the fastest-growing exponent in Eq. (30) appears in the first term, which is controlled by u_0 only. Taking this into account, we will mostly focus on variations of u_0 in what follows.

Let us first consider a solution within radiation domination, like that taking place around the fixed point I. The growing modes in this case are given by $U \rightarrow u_0$ and $V \rightarrow \frac{1}{20}e^{4N}u_0$. If we start with an initial condition $\Omega_R = 1$, the numerator of Eq. (13) tells us that the nonlocal corrections take over at $N_{\text{NL}} = -\frac{1}{4}\log(\frac{\gamma u_0}{4})$ e -foldings. Thus, the radiation-dominated Universe in the MM model is stable if and only if we have exactly the minimal boundary condition prescription.

In a realistic cosmology we should also consider a matter-dominated epoch following the radiation-domination era. This matter-dominated era happens around the critical point II. For $w_c = 0$, the inhomogeneous modes in Eqs. (29) and (30) survive and the solution is necessarily unstable. The number of e -foldings N_{NL} at which the nonlocal corrections take over is again dictated by the numerator of Eq. (13). At N_{NL} e -foldings, the sign of the fastest-growing mode is positive if¹¹

$$u_0 > -\left(\frac{10}{9} + \frac{4}{3}\log\frac{9}{5}\right) + \frac{2}{3}\log\gamma. \quad (31)$$

As we will confirm below, one should expect this sign to determine the evolution of the system beyond point II. Note that Eq. (31) can be translated into a bound on the value of $U(N_*)$ at any given number of e -foldings N_* by noticing that

$$u_0 = U(N_*) - 2\frac{(1-3w_c)N_*}{1-w_c} - \frac{4(1-3w_c)}{3(1-w_c)^2}. \quad (32)$$

In particular, for matter-radiation equality ($N_* = -8.1$), we get $U(N_*) > -15.65 + \frac{2}{3}\log\gamma$. Note that this is close to the numerical value of \bar{U} found in Eq. (28).

The above two cases constitute the only possibilities for realizing a constant equation of state $w_{\text{eff}} = w_c$ in a universe with nonvanishing and minimally coupled radiation and dust components. In what follows, we will consider vacuum solutions with $\Omega_R = \Omega_M = 0$. Combining Eqs. (13) and (15) we get

$$UV'' - 2U'V' = -\frac{3}{2}(U - w_c U + 8)V' - 12V + \frac{4}{\gamma}. \quad (33)$$

As in the nonvacuum case, the attractor solutions can be associated only to an effective equation of state $w_c = 1/3$. The fixed point V falls into this category. Indeed, when we set $u_1 = v_1 = 0$, Eq. (33) reduces to

$$e^{4N}(u_0 + 3) - \frac{\gamma}{4u_0}(1 - 3\gamma v_0) = 0, \quad (34)$$

which allows for the solutions

$$U(N) = -3, \quad V(N) = \frac{1}{3\gamma} - \frac{3}{20}e^{4N}. \quad (35)$$

Equations (35) are exact solutions of the system of Eqs. (29), (30), and (33). Note, however, that there can still be approximate solutions. Consider temporary regions with $w_c \approx -1$, as those appearing around points III and IV. In these regions, Eqs. (29) and (33) give $U'(N) \rightarrow 4$ and $V(N) = 1/(3\gamma)$, but one should be aware that Eq. (30) is only valid for a constant w_{eff} . If $U(N_{\text{NL}}) < -3$ when this solution is reached at N_{NL} , the trajectory will hit the aforementioned attractor with $w_c = 1/3$ and stay there; this is then part of what we called path B, cf. Sec. III A 2. If $U(N_{\text{NL}}) > -3$, the evolution will continue in the phase with $w_c \approx -1$ and $U' = 4$; this phase belongs to path A, cf. Sec. III A 1.

To summarize, the post-matter-dominated Universe reaches an accelerating stage with $w_c \approx -1$ which goes on until $U(N) = u_0 + 4N = -3$. If $u_0 > -3$, this period extends forever. Otherwise, one can prolong the transient acceleration for ΔN e -foldings by lowering the initial value of $U_0 \rightarrow U_0 - 4\Delta N$.

The results of this subsection are in agreement with what we studied in greater detail in the previous subsections, namely the stability analysis in the phase-space formulation and the numerical integration of the field equations.

⁹ The values u_0 and v_0 , that are set at $N = 0$ according to the solutions (29) and (30), should not in general be confused with U_0 and V_0 , the initial values for U and V set at an early radiation-dominated epoch.

¹⁰ Eqs. (29) and (30) are exact and model-independent solutions as long as we can assume that w_{eff} is a constant.

¹¹ This formula is approximate because when $\Omega_M = 1/2$, $w_c = 0$ is not exact.

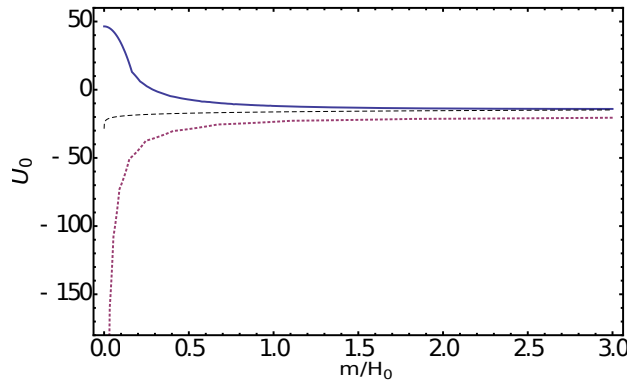


Figure 6. Value of U_0 needed to reach path A (blue curve) or path B (red dotted curve) when $\Omega_M^0 = 0.3$. For large m , the two curves converge to \bar{U} , represented by the intermediate dashed curve, which follows Eq. (28).

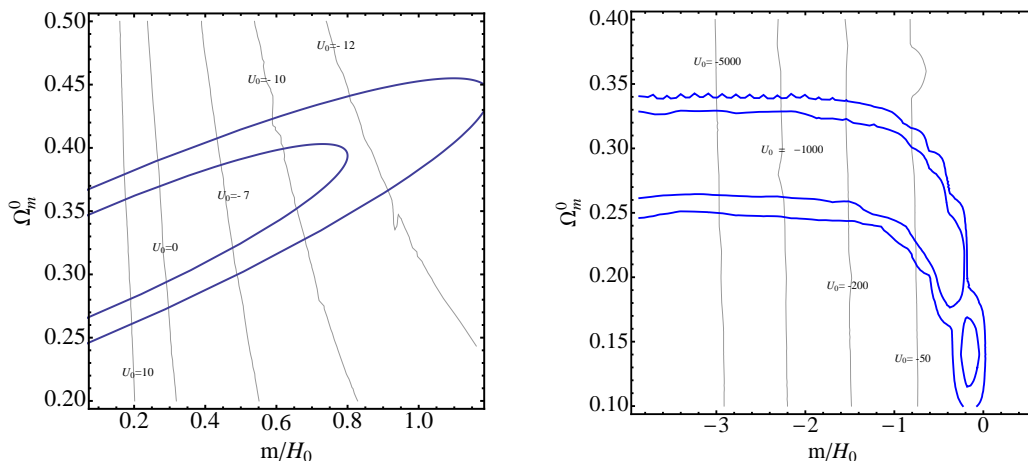


Figure 7. Supernovae likelihood contours at $2\text{-}\sigma$ level for path A (left panel) and path B (right panel). The associated values of U_0 are also displayed.

IV. CONSTRAINTS FROM SUPERNOVAE DATA

Since both paths A and B realize cosmologies that are in principle viable (i.e., they contain a sequence of proper radiation-, matter-, and dark-energy-dominated eras), we need to compare both to observations. Here, we assume as free parameters, m in units of H_0 and the present matter density parameter Ω_M^0 , and fix $\Omega_R^0 = 4.15 \cdot 10^{-5} h^{-2}$ and $V_0 = 0$. The initial condition deep in the radiation era, that we choose arbitrarily as $U_0 \equiv U(N = -14)$, is fixed by the requirement that we reach Ω_M^0 today. In practice, for every point $\{m, \Omega_M^0\}$ in the parameter space, we vary iteratively U_0 until we find Ω_M^0 at $N = 0$. Since there are two possible paths, we find two values of U_0 for every choice of parameters. The particular choice of U_0 as a function of m when $\Omega_M^0 = 0.3$ is presented in Fig. 6. For large m , paths A and B lead to a common behavior, and their initial condition U_0 also converges.

Once the two trajectories are found, we evaluate the Hubble rate $H(z)$ for each path and compare the associated luminosity distance $d_L(H(z))$ to the Joint Light-curve Analysis (JLA) supernovae data set [52] in order to obtain two independent likelihoods over m and Ω_M^0 , one for each path. When the pair $\{m, \Omega_M^0\}$ is specified, the effective equation of state w_{eff} is completely determined. The results are shown in Figs. 7 and 8. Focusing on $\Omega_M^0 \approx 0.3$, one sees that all the values of m up to 0.5 are roughly compatible with supernovae. Note, however, that the expectation value $\Omega_M^0 \approx 0.3$ comes from standard cosmology and it should not be directly applied to modified gravity cases. In fact, the supernovae data set is roughly compatible with all values of $\Omega_M^0 < 0.45$, so a more robust upper limit for m is around 1.2. For very small m , the trajectories of both path A and path B become observationally indistinguishable from Λ CDM.¹² Note, however, that this may change in the future when the dynamical part associated with nonlocal

¹² Indeed, when m is small, the dynamical part associated with nonlocal contributions in Eq. (13) is suppressed. The leading contribution

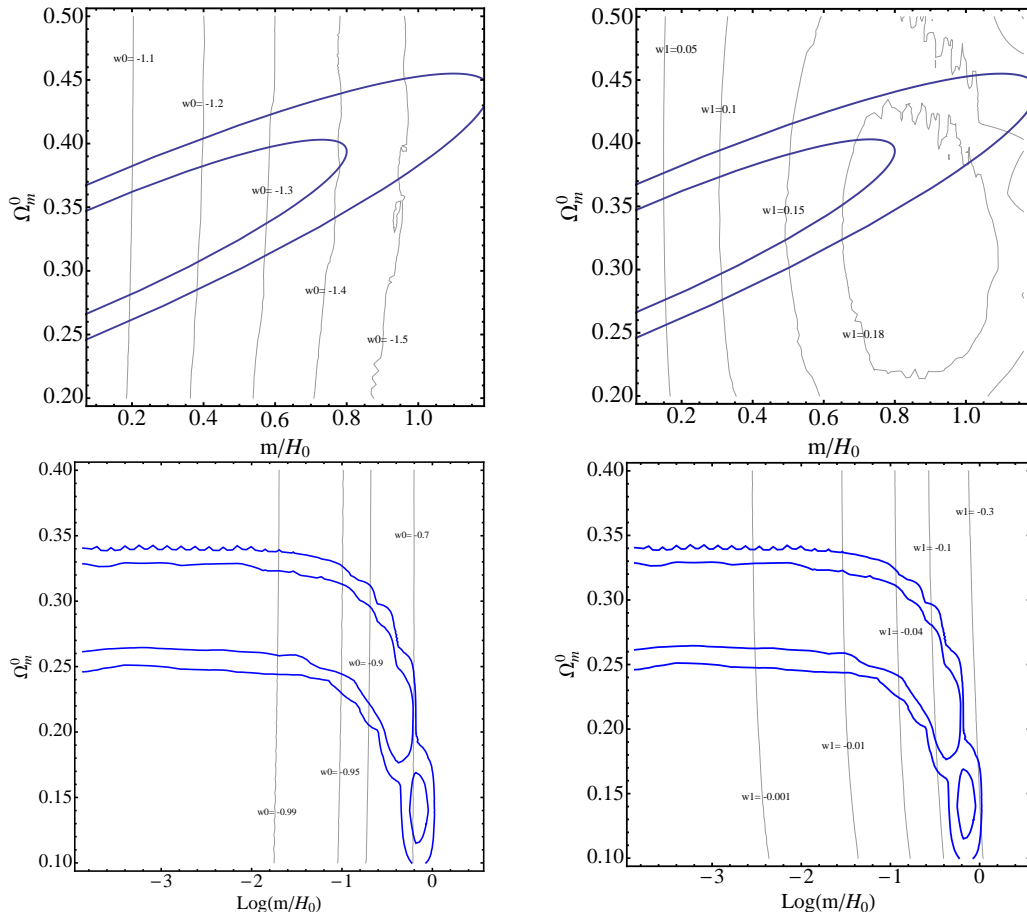


Figure 8. Supernovae likelihood contours at $2\text{-}\sigma$ level for path A (upper panels) and path B (lower panels). The associated values of w_0 and w_1 in the standard parametrization $w_{\text{eff}} = w_0 + (1 - a)w_1$ are also displayed.

contributions in Eq. (13) becomes dominant again.

V. SUMMARY AND CONCLUSIONS

Nonlocality can emerge from local theories. If one focuses on classical physics at long wavelengths, there can appear nonlocal constraints due to the effect of short wavelengths that have been integrated out. In quantum field theories, nonlocality is introduced in the computation of the effective action via the integration of the radiative corrections due to massless or light particles.

It is thus natural to consider that nonlocal, infrared modifications of gravity at cosmological scales, such as in the model described by (2), could provide a useful effective approach to study the problems of cosmological constant and of dark energy. An important subtlety, not arising in local modifications of gravity, has to then be taken into account in such studies: in addition to the mass parameter in the Lagrangian (2), the nonlocal model is understood to be specified by the boundary conditions implied by the presence of the inverse-d'Alembertian.

In this work, we have considered the effect of general initial conditions on the dynamical system (22)-(27) for the background evolution of the $R\Box^{-2}R$ cosmological model, as well as the constraints from supernovae data on the parameters m and Ω_M^0 . The system exhibits two distinct classes of late-time behavior, which lead to two different types of cosmological evolution, dubbed path A and path B.

Path A (path B) is realized above (below) a certain threshold \bar{U} for the initial condition of the auxiliary field U , U_0 . The case $U_0 = 0$, belonging to path A, is the one already discussed in Ref. [32]. Note, however, that the initial

at early times is of order mU_{hom} , which is a constant in our case. Note that this is in agreement with the curve corresponding to path B in Fig. 6.

conditions in this theory are sensitive to the thermal history of the Universe. In particular, the value of U at a given number of e -foldings cannot be unambiguously set to zero by setting $U_{\text{hom}} = 0$. The main result of this work is to extend the cosmological analysis to the full range of initial conditions.

We found that although both paths possess well-behaved radiation and matter eras, the subsequent evolution is in general radically different. Along path A, the system goes through a phantom regime and finally reaches an attractor on which the effective equation of state w_{eff} remains frozen at the CC value -1 . This final state, however, is not a de Sitter stage since H (and therefore the Ricci scalar R) is not constant, but rather grows indefinitely. Along path B, instead, the evolution remains always nonphantom; the system reaches generically a $w_{\text{eff}} = -1$ stage which approaches a true de Sitter stage. This is however a temporary stage in cosmic evolution, as the solution is not an attractor but, rather, a saddle point. After a transient period the system reaches a final configuration represented by a decelerated, radiationlike, $w_{\text{eff}} = 1/3$ state (and therefore with $R = 0$), in which, however, no radiation is present. The present value of the nonlocal-term equation of state, w_{DE} , can take essentially any values around -1 . The impact of initial conditions on the final evolution is therefore important.

Both paths are in principle cosmologically viable. When compared to supernovae observations, we find the regions in the $\{m, \Omega_M\}$ parameter space that satisfy observational constraints. It is interesting to note that small, even vanishing, values of m are perfectly acceptable. This means that cosmologically viable nonlocal terms can be generated from standard loop corrections, which require $m/H_0 \ll 1$ (in Planck units). However, in this case the evolution becomes indistinguishable from Λ CDM.

The methods employed in this paper can be applied to more general nonlocal models. We saw that the possible cosmological dynamics of a given model can be conveniently derived from the behavior of the additional scalar modes carried by the nonlocal integral operators. Assuming a background evolution with a power-law expansion of the scale factor, we solved for the mode functions in the model (2), and from the general solutions (29) and (30) deduced the handful of fixed points and their basic properties. A similar analysis should be even more transparent for actions of the type (1), since there the nontrivial modes are given solely by Eq. (29). In models featuring the conformal Weyl curvature [18, 28, 29], a substantial simplification is that only the homogeneous modes are nonvanishing.

In conclusion, the cosmological background dynamics of the nonlocal model studied here depend qualitatively upon the initial conditions. We discussed the initial conditions in terms of U_0 set at an early radiation-dominated epoch and showed that different values for this parameter can result in the Universe ending up eventually in drastically different stages: in the two most typical cases studied here, either a phantomlike approach towards asymptotic singularity, or an eternal conformal expansion. The initial value $U_0 = 0$ is a natural choice, but its implementation in fact depends on the thermal history of the Universe. As shown in Appendix B, however, the ambiguity is not large enough to change the evolution from the former track to the latter.

We can thus regard the interesting dark energy behavior as a robust background prediction of the model (2). It remains to be seen whether one can learn further about the structure formation in nonlocal cosmology by revisiting the boundary conditions of the integral operators at the level of the inhomogeneous perturbation modes.

ACKNOWLEDGMENTS

We thank Florian Führer and Adam R. Solomon for helpful discussions. We also acknowledge support from DFG through the project TRR33 “The Dark Universe.” H.N. also acknowledges financial support from DAAD through the program “Forschungsstipendium für Doktoranden und Nachwuchswissenschaftler.”

Appendix A: Some clarifications on fixed points and paths

1. From fixed surfaces to fixed points

As explained in Sec. III A, when the first derivative of a variable on the left-hand side of Eqs. (22)-(27) takes a constant value, the dynamical system contains a fixed surface rather than a fixed point. To illustrate how to deal with this situation, we present below the complete phase-space analysis for the critical point II in Table I. A similar analysis can be done for points III and IV.

As follows directly from Eq. (22), when $Y_1 = 2$ the variable U satisfies the equation of a line, $U' = 2$. In order to go from this fixed line to a fixed point we can consider a field redefinition,

$$U = \tilde{U} + 2N, \quad (\text{A1})$$

with N the number of e -foldings. Inserting this relation into Eqs. (22)-(27), one immediately realizes that $Y_1 = 2$ corresponds to a fixed point $\tilde{U}' = 0$. Written in the new variables, the analysis proceeds along the lines discussed in

Sec. III A. The behavior of the system around the fixed point is determined by the eigenvalues of the characterizing matrix, which are given by

$$\lambda_i = \left\{ 0, 0, -1, -\frac{3}{2}, -\frac{3}{2}, \frac{3\tilde{U}_0 + 6N + 4}{\tilde{U}_0 + 2N} \right\}, \quad (\text{A2})$$

with \tilde{U}_0 an arbitrary constant. From the theory of dynamical systems we know that the so-called Lyapunov coefficients s_i ($i = 1, 2, \dots, 6$) are equal to the real part of the eigenvalues λ_i , provided that these eigenvalues are constant. Note however that, due to the field redefinition (A1), the last eigenvalue in Eq. (A2) depends on the number of e -foldings N . The Lyapunov coefficient in this case is defined by the upper limit

$$s_6 = \lim_{N \rightarrow \infty} \frac{1}{N - N_0} \int_{N_0}^N \text{Re}\{\lambda_6(N')\} dN', \quad (\text{A3})$$

with N_0 some initial value for N . Taking into account (A2), we get

$$s_6 = \lim_{N \rightarrow \infty} \frac{1}{N - N_0} \int_{N_0}^N \frac{3\tilde{U}_0 + 6N' + 4}{\tilde{U}_0 + 2N'} dN' = 3. \quad (\text{A4})$$

The resulting spectrum of Lyapunov coefficients

$$s_i = \left\{ 0, 0, -1, -\frac{3}{2}, -\frac{3}{2}, 3 \right\} \quad (\text{A5})$$

shows that the fixed point under consideration is a saddle point.

2. On the two realizations of the fixed point V

Note that point V in Table I has two different realizations. The first one is obtained for $V = +\infty$ and $\Omega_M = -\infty$, while the second case corresponds to $V = -\infty$ and $\Omega_M = +\infty$. In this Appendix, we discuss the set of initial conditions giving rise to each one of these configurations.

Around the fixed point V, we have $U' = U'' = 0$. These two conditions restrict the ξ parameter in Eq. (14) to a fixed value $\xi = -2$. Inserting this constant value into Eq. (15) and taking into account the large N limit of Eq. (13), we get

$$V'' - 3V' - 4V + \frac{4}{3\gamma} = 0. \quad (\text{A6})$$

For $N \gg 1$, the solution of this differential equation reads

$$V \approx \frac{1}{3\gamma} + \left(V_0 - \frac{1}{3\gamma} + V'_0 \right) e^{4(N-N_0)}, \quad (\text{A7})$$

with V_0 and V'_0 the values of V and V' at some initial time N_0 . In view of this solution, we can distinguish two possibilities. If $V_0 > 1/(3\gamma) - V'_0$, the system approaches the fixed point V with $V \rightarrow +\infty$.¹³ In the opposite case, the fixed point V is realized with $V \rightarrow -\infty$.

Appendix B: Initial conditions and thermal history of the Universe

In this Appendix we estimate the robustness of the MM initial conditions when the detailed particle content of the Universe prior to matter-radiation equality is taken into account.

For some purposes, the transition from radiation to matter domination can be approximated by an instant transition at $N_{\text{eq}} \simeq -8.1$ in which the trace of the energy-momentum tensor changes abruptly from zero to $e^{3N_{\text{eq}}}$ times its present

¹³ Note that realizations with $V_0 > 1/(3\gamma) - V'_0$ are not physically acceptable. As can be easily deduced from Eq. (13), these configurations give rise to negative values of h^2 around the fixed point V.

value. This approximation implicitly assumes that all the particles in the early Universe have roughly the same mass, and transit simultaneously from a relativistic to a nonrelativistic state. A detailed analysis of the thermal history of the Universe allows us to go beyond this approximation and to account for the fact that particles with different masses become nonrelativistic at different temperatures, or equivalently, at different cosmic times.

The change in the trace of the energy-momentum tensor can be parametrized as

$$\text{tr}(T_{\mu\nu}) = \frac{\rho - 3P}{M_{\text{Pl}}^2} \equiv \frac{\rho_{\text{R}}}{M_{\text{Pl}}^2} \Sigma(T), \quad (\text{B1})$$

with T and ρ_{R} the temperature and energy density of the radiation bath.¹⁴ The so-called “kick” function $\Sigma(T)$ is computed by summing the individual contributions to the bath of the particles with mass m_i , temperature T_i and g_i degrees of freedom [53],¹⁵

$$\Sigma_i(T) = \frac{\rho_i - 3p_i}{\rho_i} = \frac{15}{\pi^4} \frac{g_i}{g_*(T)} \left(\frac{m_i}{T}\right)^2 \int_{m_i/T}^{\infty} \frac{\sqrt{u^2 - (m_i/T)^2}}{e^u \pm 1} du, \quad (\text{B2})$$

where $g_*(T) \equiv \rho_{\text{R}}[(\pi^2/30)T^4]^{-1}$ is the total number of relativistic degrees of freedom in the bath.

Equation (B1) translates, via Einstein equations, into a change of the Ricci scalar, $R = \text{tr}(T_{\mu\nu})$. Integrating Eq. (9) with $a(t) \simeq t^{1/2}$ and taking into account the relation between time and temperature at radiation-domination,

$$t \simeq \sqrt{\frac{45}{2\pi^2} g_*^{-1/2} \frac{M_{\text{Pl}}}{T^2}}, \quad (\text{B3})$$

we get

$$\Delta U \equiv U - U_{\text{hom}} = \frac{45}{2\pi^2} M_{\text{Pl}}^2 \int_{T_i}^{T_f} dT' \mathcal{D}(T') g_*^{1/4}(T') T' \times \int_{T_i}^{T'} dT'' \mathcal{D}(T'') \frac{R(T'')}{(T'')^5 g_*^{5/4}(T')}, \quad (\text{B4})$$

with

$$\mathcal{D}(T) \equiv \left(-\frac{2}{T} - \frac{1}{2g_*(T)} \frac{\partial g_*(T)}{\partial T} \right). \quad (\text{B5})$$

Here, T_i and T_f are the higher and lower temperatures for which radiation domination is a reasonable first order approximation for the background evolution of the Universe. Note that, due to the integration between T_i and T_f , even a tiny value of the scalar curvature at early times ($T_f \ll T_i$) can give rise to a sizable modification of U at matter-radiation equality.¹⁶

The radiation-domination requirement ($R = 0$) giving rise to the MM initial conditions should be understood only as an approximation of the actual dynamics. The value of U at radiation domination cannot be unambiguously set to zero by simply setting $U_{\text{hom}} = 0$. Indeed, if the initial conditions are set at the end of inflation/reheating, one should expect nonvanishing values of U_0 at the number of e -foldings at which the MM initial conditions are usually implemented ($N \simeq -14$). Note also that, even if the MM initial conditions are taken for granted, the detailed thermal history of the Universe will inevitably affect the subsequent evolution of U . The uncertainty associated to this effect depends on the particle content of the early Universe. Assuming radiation domination between 1000 GeV and 0.75 eV and considering only the contribution of Standard Model particles, we can numerically integrate Eq. (B4) to obtain a correction

$$\Delta U \approx 1.6, \quad (\text{B6})$$

to be added on top of the nonvanishing MM value at matter-radiation equality [35]. The assumptions leading to the uncertainty (B6) are indeed quite conservative. Larger values of ΔU should be expected if we accept the existence of new physics beyond the Standard Model.

[1] L. Amendola and S. Tsujikawa, Dark Energy: Theory and Observations (Cambridge University Press, New York, 2010).

¹⁴ Note that if all the particles prior to recombination were completely massless, $\Sigma(T)$ would be zero.

¹⁵ The + and – signs in the denominator of the integrand apply, respectively, to fermions and bosons.

¹⁶ For $T_i \gg T_f$ and constant values of g_* and Σ we have

$$\Delta U \sim \Sigma \int_{T_i}^{T_f} dT' \int_{T_i}^{T'} dT'' \frac{1}{(T'')^2} \sim \Sigma \left[\ln \frac{T_i}{T_f} - \frac{T_i - T_f}{T_i} \right] \sim \Sigma \ln \frac{T_i}{T_f}.$$

- [2] P. Bull, Y. Akrami, et al., *Phys. Dark Univ.* **12**, 56 (2016), 1512.05356.
- [3] R. P. Woodard, *Found. Phys.* **44**, 213 (2014), 1401.0254.
- [4] A. O. Barvinsky, *Mod. Phys. Lett.* **A30**, 1540003 (2015), 1408.6112.
- [5] W. Siegel (2003), hep-th/0309093.
- [6] G. Calcagni and L. Modesto, *Phys. Rev.* **D91**, 124059 (2015), 1404.2137.
- [7] T. Biswas, T. Koivisto, and A. Mazumdar, in *Proceedings, Barcelona Postgrad Encounters on Fundamental Physics, Barcelona (2013)*, pp. 13–24, 1302.0532.
- [8] T. Biswas, E. Gerwick, T. Koivisto, and A. Mazumdar, *Phys. Rev. Lett.* **108**, 031101 (2012), 1110.5249.
- [9] L. Modesto, *Phys. Rev.* **D86**, 044005 (2012), 1107.2403.
- [10] A. Codello and R. K. Jain (2015), 1507.06308.
- [11] J. F. Donoghue and B. K. El-Menoufi, *JHEP* **10**, 044 (2015), 1507.06321.
- [12] C. Wetterich, *Gen. Rel. Grav.* **30**, 159 (1998), gr-qc/9704052.
- [13] A. O. Barvinsky, *Phys. Rev.* **D85**, 104018 (2012), 1112.4340.
- [14] M. Jaccard, M. Maggiore, and E. Mitsou, *Phys. Rev.* **D88**, 044033 (2013), 1305.3034.
- [15] L. Modesto and S. Tsujikawa, *Phys. Lett.* **B727**, 48 (2013), 1307.6968.
- [16] G. Cusin, J. Fumagalli, and M. Maggiore, *JHEP* **09**, 181 (2014), 1407.5580.
- [17] A. Golovnev, T. Koivisto, and M. Sandstad, *Phys. Rev.* **D93**, 064081 (2016), 1509.06552.
- [18] T. Koivisto and F. Koennig (to be published).
- [19] T. Padmanabhan, *J. Phys. Conf. Ser.* **701**, 012018 (2016).
- [20] S. Deser and R. P. Woodard, *Phys. Rev. Lett.* **99**, 111301 (2007), 0706.2151.
- [21] T. Koivisto, *Phys. Rev.* **D77**, 123513 (2008), 0803.3399.
- [22] C. Deffayet and R. P. Woodard, *JCAP* **0908**, 023 (2009), 0904.0961.
- [23] E. Elizalde, E. O. Pozdeeva, and S. Yu. Vernov, *Class. Quant. Grav.* **30**, 035002 (2013), 1209.5957.
- [24] T. S. Koivisto, *Phys. Rev.* **D78**, 123505 (2008), 0807.3778.
- [25] A. Conroy, T. Koivisto, A. Mazumdar, and A. Teimouri, *Class. Quant. Grav.* **32**, 015024 (2015), 1406.4998.
- [26] S. Dodelson and S. Park, *Phys. Rev.* **D90**, 043535 (2014), 1310.4329.
- [27] P. G. Ferreira and A. L. Maroto, *Phys. Rev.* **D88**, 123502 (2013), 1310.1238.
- [28] G. Cusin, S. Foffa, M. Maggiore, and M. Mancarella, *Phys. Rev.* **D93**, 043006 (2016), 1512.06373.
- [29] G. Cusin, S. Foffa, M. Maggiore, and M. Mancarella, *Phys. Rev.* **D93**, 083008 (2016), 1602.01078.
- [30] M. Maggiore and M. Mancarella, *Phys. Rev.* **D90**, 023005 (2014), 1402.0448.
- [31] Y. Dirian and E. Mitsou, *JCAP* **1410**, 065 (2014), 1408.5058.
- [32] Y. Dirian, S. Foffa, M. Kunz, M. Maggiore, and V. Pettorino, *JCAP* **1504**, 044 (2015), 1411.7692.
- [33] A. Codello and R. K. Jain (2015), 1507.07829.
- [34] A. Codello and R. K. Jain (2016), 1603.00028.
- [35] Y. Dirian, S. Foffa, N. Khosravi, M. Kunz, and M. Maggiore, *JCAP* **1406**, 033 (2014), 1403.6068.
- [36] S. Nesseris and S. Tsujikawa, *Phys. Rev.* **D90**, 024070 (2014), 1402.4613.
- [37] A. Barreira, B. Li, W. A. Hellwing, C. M. Baugh, and S. Pascoli, *JCAP* **1409**, 031 (2014), 1408.1084.
- [38] Y. Dirian, S. Foffa, M. Kunz, M. Maggiore, and V. Pettorino (2016), 1602.03558.
- [39] M. Maggiore, *Phys. Rev.* **D93**, 063008 (2016), 1603.01515.
- [40] S. Foffa, M. Maggiore, and E. Mitsou, *Int. J. Mod. Phys.* **A29**, 1450116 (2014), 1311.3435.
- [41] A. Kehagias and M. Maggiore, *JHEP* **08**, 029 (2014), 1401.8289.
- [42] R. P. Woodard, *Phys. Rev.* **A62**, 052105 (2000), hep-th/0006207.
- [43] N. Barnaby and N. Kamran, *JHEP* **12**, 022 (2008), 0809.4513.
- [44] T. S. Koivisto, *AIP Conf. Proc.* **1206**, 79 (2010), 0910.4097.
- [45] N. Barnaby, *Nucl. Phys.* **B845**, 1 (2011), 1005.2945.
- [46] G. Calcagni and G. Nardelli, *Phys. Rev.* **D82**, 123518 (2010), 1004.5144.
- [47] S. Foffa, M. Maggiore, and E. Mitsou, *Phys. Lett.* **B733**, 76 (2014), 1311.3421.
- [48] N. C. Tsamis and R. P. Woodard, *JCAP* **1409**, 008 (2014), 1405.4470.
- [49] Y.-l. Zhang, K. Koyama, M. Sasaki, and G.-B. Zhao, *JHEP* **03**, 039 (2016), 1601.03808.
- [50] E. Calzetta and B. L. Hu, *Phys. Rev.* **D35**, 495 (1987).
- [51] R. D. Jordan, *Phys. Rev.* **D33**, 444 (1986).
- [52] M. Betoule et al. (SDSS), *Astron. Astrophys.* **568**, A22 (2014), 1401.4064.
- [53] A. L. Erickcek, N. Barnaby, C. Burrage, and Z. Huang, *Phys. Rev.* **D89**, 084074 (2014), 1310.5149.